Int. J. Multiphase Flow Vol. 8, No. 3, pp. 227–238, 1982
Printed in Great Britain.

0301-9322/82/030227-12$03.00/0
Pergamon/Elsevier

DROPLET DEPOSITION ON A FLAT PLATE FROM AN AIR/WATER TURBULENT MIST FLOW

M. TRELA, J. ZEMBIK and B. DURKIEWICZ

Institute of Fluid Flow Machines, Polish Academy of Sciences, ul. Gen. J. Fiszera 14, 80-952 Gdansk, Poland

(*Received* 20 *June* 1980; *in revised form* 24 *August* 1981)

Abstract—A model of droplet deposition from a turbulent gas flow on a vertical plate is presented. It is based on the stopping distance concept, allowing for the different turbulent diffusivities of the gas and the droplets. The experimental apparatus is described and the obtained results are presented. Comparison between the presented theory and some of the existing experimental data shows satisfactory agreement.

1. INTRODUCTION

Solid or liquid particle deposition from a turbulent gas flow on boundary surfaces has been a subject of investigation for many years because of its importance in a number of engineering problems. In spite of this, the phenomenon has not been sufficiently understood, particulary for particles larger than 1 μm dia the deposition of which is controlled by the particle size and the gas flow turbulence.

A wide review of pertinent bibliography is presented *b* by McCoy & Hanratty (1977). The authors set available experimental results in the form of dimensionless deposition coefficient k/u^* vs the dimensionless particle stopping distance S^+. The deposition coefficient k expressed in m/s is defined by the relationship

$$m = k\bar{c} \qquad [1]$$

where m stands for the mass flux of deposited particles and $\bar{c}$ is the mean particle concentration within the duct. A dimensionless form of this coefficient is obtained by normalizing it with respect to the friction velocity u^*. The stopping distance for a particle of diameter d_p obeying a Stokesian drag relation and having an initial velocity $u_0 = u^*$ is equal to

$$S = \frac{\rho_p d_p^2 u^*}{18\mu_G} \qquad [2]$$

where ρ_p is the density of the particle and μ_G is the gas dynamic viscosity. Hence, the dimensionless stopping distance is

$$S^+ = \frac{Su^*\rho_G}{\mu_G} = \frac{d_p^2 u^{*2}\rho_G^2\rho_p}{18\mu_G^2\rho_G} \qquad [3]$$

where ρ_G is the density of the gas. A discussion of the assumptions used to determine the stopping distance is given in appendix A.

Following the McCoy & Hanratty (1977) survey one may distinguish three different deposition ranges with different deposition modes.

The first range concerns very small particles with $S^+ < 0.15$. Particle deposition within this range is controlled by the molecular diffusion process.

In the second range, for $0.15 < S^+ < 22.9$, the mass flux of deposited particles is a result of a complex gas-particle interaction. The trajectories of the particles become influenced by their inertia. The particle deposition coefficient within this range rises very rapidly with increasing stopping distance S^+.

Finally, the third range covers the large particle deposition with $S^+ > 22.9$. In this case the coefficient k/u^* seems to be independent of the stopping distance S^+, thus suggesting the inertial deposition prevails. Sufficient understanding of this deposition mechanism is important in practice since this type of deposition is very often encountered in different gas-droplet flows.

A number of investigations is devoted to droplet deposition on the duct walls. Among those widely known are experimental studies of Alexander & Coldren (1951), Cousins & Hewitt (1968), Namie & Ueda (1972). Theoretical analyses were performed, among others, by Hutchinson *et al.* (1971), Namie & Ueda (1973).

Droplet deposition on a horizontal plate placed in a wind tunnel was investigated by Simpson & Brolls (1974). The authors suggested a droplet deposition model based on the assumed analogy between heat and mass transfer processes.

Trela (1980) performed the theoretical analysis of the droplet deposition on a vertical plate, using the stopping distance concept and allowing for different turbulent diffusivities of the gas and the droplets.

This paper presents the above analysis together with the results of the experimental investigation of droplet deposition on the vertical plate.

2. THEORETICAL ANALYSIS

The analysis is restricted to deposition of droplets from fully developed turbulent gas flow on a vertical plate placed in a duct. The concentration of droplets in the stream is small enough to neglect its effect on turbulent fluid properties. Once the droplets strike the surface there is assumed to be no rebound or re-entrainment. Brownian motion, electrostatic, lift and thermal forces are to be neglected. The lift force had been usually neglected until Rouhiainen & Stachiewicz (1970) pointed to its significant role in the deposition of small particles. However, for larger particles this effect is diminished in favour of inertia force. A similar conclusion may be drawn from the paper of Ganic & Rohsenow (1979). Hence, the lift force is neglected in this analysis concerning the large droplets.

According to the theory of turbulent motion, the size and angular frequency of the turbulent eddies depend on the distance from the wall, in such a manner, that towards the wall their size diminishes and their frequency increases. While the droplets in the turbulent core approximately follow the stream motion when approaching the wall they enter the region of high frequency eddies where, due to the droplet inertia, their diffusivities drop to zero. The droplets become insensitive to the gas velocity fluctuation and thus droplets sufficiently large may penetrate into this region thanks their velocity impulse gained at the edge of this region.

If at the edge of this region the concentration of the droplets is C, the mean y-directional particle velocity fluctuation imparted by the gas transverse velocity fluctuation is v_p', then the mass flow rate of the droplets depositing on the wall can be written as

$$m = Pv_p'c \qquad [4]$$

where P is a deposition probability or the fraction of droplets getting the impulse toward the wall, y is the distance from the wall. Deposition in circular channals is mainly controlled by the radial droplet velocity fluctuations, thus P equals 0.5 (see appendix 2). In the model under consideration the region where the droplet diffusivity drops to zero is assumed to have a thickness equal to the stopping distance S^+.

The stopping distance concept postulated first by Friedlander & Johnstone (1957) assumed equal diffusivities of both the gas and the droplets. This assumption was criticized by Rouhiainen & Stachiewicz (1970), who showed after Tchen (Hinze 1959) that the turbulent eddy diffusivity of a droplet larger than 1 μm dia. is substantially lower than the gas eddy diffusivity.

After Tchen the ratio of eddy diffusivities may be written as

$$\frac{\epsilon_p}{\epsilon_G} = \frac{v_p'^2}{v_G'^2} = \frac{\int_0^\infty \eta^2 E_G(\omega)\,d\omega}{\int_0^\infty E_G(\omega)\,d\omega} = b \qquad [5]$$

where ϵ_p, ϵ_G are eddy diffusivities of the particles and of the gas, v_G' is the y-directional mean gas velocity fluctuation, η is the ratio between amplitudes of oscillation of particle and gas, $E_G(\omega)$ is the Langrangian energy spectrum of velocity fluctuations, ω is the angular frequency. Based on the experiments of Comte-Bellot (1965) on spectral energy distribution in turbulent flow, Namie & Ueda (1973) determined after [5] the ratio $\epsilon_p/\epsilon_G = b$ for water droplets, at the distance $2y/D = 0.42$ from the wall, where D stands for the duct diameter. Their results are shown in figure 1. versus the duct Reynolds number. Accordingly to [5] the mean droplet velocity fluctuation may be expressed as

$$v_p' = v_G'\sqrt{b} \qquad [6]$$

Both factors on the right depend on the distance from the wall. From the calculations done by Namie & Ueda ((1973) figure 13) it is seen that for droplets larger than about 10 μm dia. the ratio ϵ_p/ϵ_G varies over the duct similarly to the turbulent velocity. Hence, by analogy to the turbulent velocity distribution the power law distribution of the ratio ϵ_p/ϵ_G is postulated.

$$b = b_c\left(\frac{2y}{D}\right)^{1/n} \qquad [7]$$

with b_c standing for ϵ_p/ϵ_G on the duct axis (figure 1). The exponent n in [7] is a function of the Reynolds number and may be determined after Schlichting (1955).

The next problem to be discussed is the velocity fluctuation v_G' within the duct. After Hinze ((1959), figure 7.32 and 7.34) the ratio v_g'/u^* equals 0.715 on the duct axis, rises towards the wall, at $2y/D = 0.1$ reaches its maximum equal to 1.12 and then falls to zero at the wall. At the

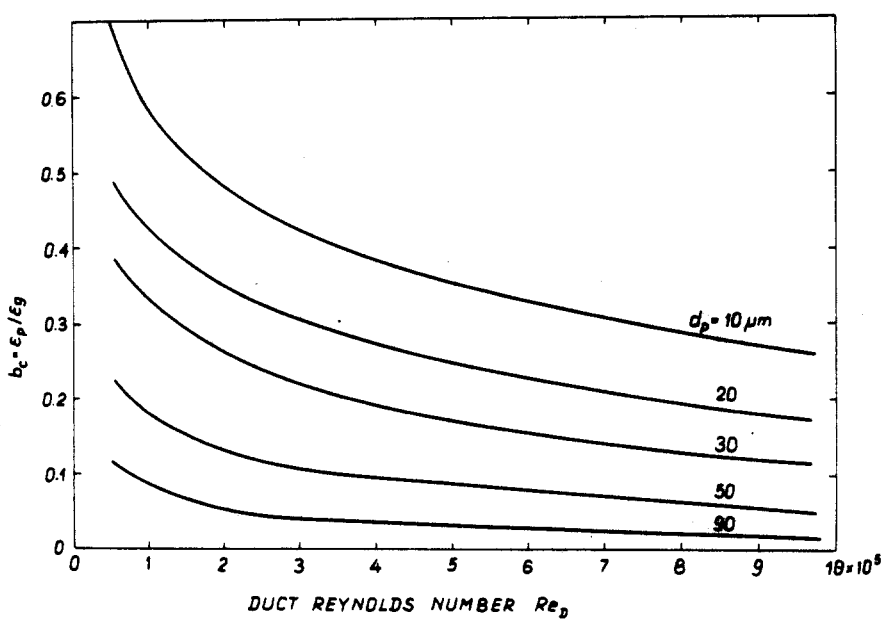

Figure 1. Ratio of eddy diffusivities after Namie and Ueda (1973).

distance $y^+ = yu^*\rho_G/\mu_G = 30$ there is $v'_G/u^* \simeq 0.7$. Thus it is seen that except for the region adjacent the wall, v'_G/u^* does not vary strongly. Accordingly the velocity fluctuation v'_G may be written as

$$v'_G = Au^* \tag{8}$$

where A is a coefficient dependent on the distance from the wall and varies within 0.7 and 1.12.

In order to determine the mass flux of depositing droplets the concentration of droplets at one stopping distance from the wall should be evaluated. Since turbulent momentum and mass transfer are accomplished by the eddies it seems reasonable to assume the concentration distribution of droplets similar to the velocity distribution in the turbulent core, i.e. for $s \leq y \leq D/2$ (see appendix C).

Therefore it is assumed that

$$\frac{c}{c_c} \simeq \frac{u}{u_c} = \left(\frac{2y}{D}\right)^{1/n} \tag{9}$$

where index c denotes values on the duct axis. Based on the above assumption the ratio of the average concentration in the channel to the maximum concentration on the axis is given as

$$\frac{\bar{c}}{c_c} = \frac{2n^2}{(n+1)(2n+1)} = B \tag{10}$$

Transforming [4] with the help of [6]–[10] one gets the mass flux expressed as

$$m = 0.5\frac{Au^*}{B}\left(\frac{2y}{D}\right)^{1.5/n}\sqrt{b_c}\,\bar{c} \tag{11}$$

from which the transfer coefficient k/u^* appears to be

$$\frac{k}{u^*} = \frac{m}{\bar{c}u^*} = 0.5\frac{A}{B}\left(\frac{2y}{D}\right)^{1.5/n}\sqrt{b_c}. \tag{12}$$

The above equation determines the dimensionless deposition coefficient k/u^* for a vertical plate situated at the distance y from the wall. For the plate placed at the duct centre

$$\frac{k_c}{u^*} = 0.5\frac{A_c}{B}\sqrt{b_c}. \tag{13}$$

For the duct Reynolds number $\mathrm{Re}_D = \bar{u}D\rho_G/\mu_G = 5 \times 10^4$ to 2×10^5 the value of the exponent n in [9] and [10] is about 7 after Schlichting (1955), thus following [10] coefficient $B = 0.816$. For the plate situated at the duct centre, where $A_c \simeq 0.715$ a simple relation holds

$$\frac{k_c}{u^*} = 0.44\sqrt{b_c}. \tag{14}$$

The model described above accounts for the variations of the deposition coefficient k in the duct. Following [12] and [13] one obtains

$$\frac{k}{k_c} = \frac{A}{A_c}\left(\frac{2y}{D}\right)^{1.5/n}. \tag{15}$$

Since, as mentioned above, beyond the wall adjacent region $A/A_c > 1$, [15] suggests a slight maximum in the ratio k/k_c. Nevertheless, for the region $0.1 < 2y/D < 1$ this ratio may be assumed practically constant and equal to 1. When the plate is moved towards the duct wall and finally coincides with it the ratio of the deposition coefficients becomes

$$\frac{k_w}{k_c} = \frac{A_s}{A_c}\left(\frac{2s}{D}\right)^{1.5/n} \qquad [16]$$

since in this case the model assumes $y = S$. In the above, index w denotes values on the duct wall and index S value at the distance S from the wall.

It should be noted that the analysis concerns the local values of the coefficient k. For the plate, the average value of the coefficient k, may be obtained by integrating the basic equation [12] with respect to the plate height.

3. EXPERIMENTAL APPARATUS

The experiments were performed on the apparatus shown schematically in figure 2. Two-phase air–water droplets mixture was produced by four pneumatic nozzles supplied with water and air at constant 2×10^5 Pa pressure. The nozzles were uniformly mounted in the tunnel walls of 0.344×0.395 m in size. The air flow was blown by a fan at a rate measured by an Alcock laminar flow meter placed at the air intake. The deposition investigation were done on a vertical plate with the height $H = 0.15$ m and the length $L = 0.3$ m placed 4.28 m away from the nozzles. The droplets deposited onto the plate formed a continuous film there which was drained to the collection flask outside the tunnel. The experiments were carried out at the two-phase medium temperature $t = 9$–11°C. The main measured quantities were: droplet deposition rate m, mean droplet concentration $\bar{c}$, mass flow rate of the air W_G, mass deposition rate on the tunnel walls W_{LF}, pressure drop in the tunnel, mass flow rate of water injected into the tunnel W_L and droplet size distribution.

The mean droplet concentration was calculated as

$$\bar{c} = \frac{W_{LE}}{W_{LE}/\rho_L + W_G/\rho_G} \qquad [17]$$

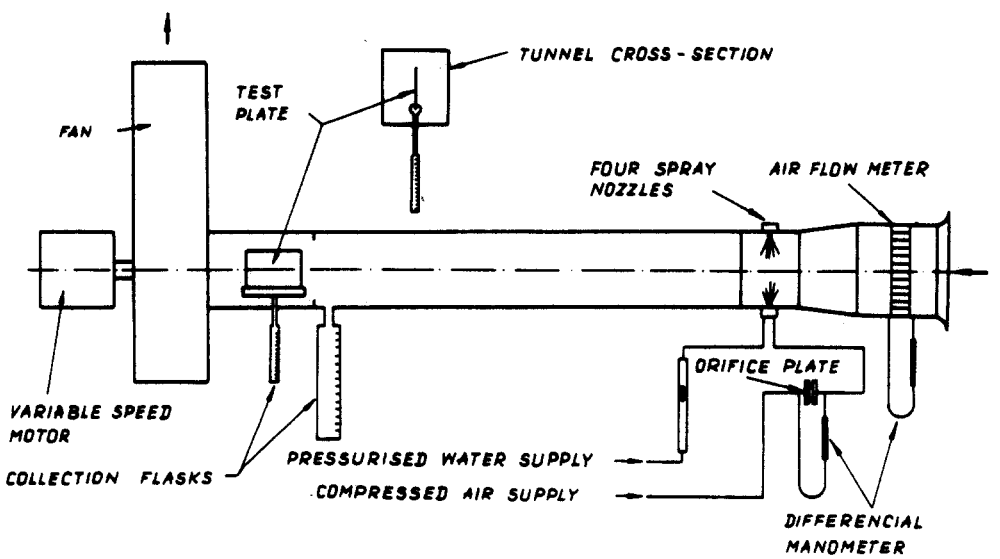

Figure 2. General arrangement of the test rig.

where W_{LE} is the mass flow rate of entrained droplets, ρ_L is the density of water. The mass flow rate W_{LE} was determined as

$$W_{LE} = W_L - W_{LF} - W_G(X_n - X_0) \quad [18]$$

where X_0 and X_n are air humidities at initial and final mist conditions. Droplet size measurement was made by means of magnesium oxide coated slides with a special slide holder.

The deposition investigations were performed at the mean velocity in the duct $\bar{u}$ = 1–14.1 m/s and corresponding Reynolds number $Re_D = \bar{u}D\rho_G/\mu_G$ = 25 000–360 000 based on the duct hydraulic diameter D = 0.365 m. The maximum droplet concentration during these investigations reached 0.035 kg/m^3.

The investigations were always started from the maximum air velocity thus assuring rapid wetting of the plate and stabilization of the film flow over the tunnel walls. The experiments were continued only with the film entirely wetting the plate.

Otherwise, if dry spots appeared, the experiments were stopped and the plate carefully cleaned.

4. RESULTS AND DISCUSSION

The experiments were carried out in two stages. In the first velocity profiles, intensity of turbulence, friction factor of the tunnel, droplet size measurement and the droplet deposition onto the vertical plate situated at the tunnel centre were investigated. The pressure drop measurements of dry air flow revealed a very high roughness of the tunnel resulting in the ratio of Fanning friction factors, $f/f_s \simeq 100$. The smooth tube friction factor f_s was determined from the Blasius formula

$$f_s = 0.0791\, Re_D^{-0.25} \quad [19]$$

It was also used to calculate the friction velocity

$$u^* = \bar{u}\sqrt{f_s/2} \quad [20]$$

over the entire range of the experiments.

An example of the velocity profiles and turbulence level measurements is shown in figure 3. They were done by means of DISA 55M anemometer system. An example of droplet size distribution for one selected air flow velocity is shown in figure 4. Moreover, figure 5 shows the mean droplet diameter distribution (arithmetic diameter d_{10}, volumetric diameter d_{30} and Sauter diameter d_{32}) vs air velocity. Finally, the main droplet deposition results are plotted in figure 6.

The second stage of experiments cover droplet deposition measurements on the vertical plate placed at the tunnel center and at a distance y = 0.063 m from the side wall. The measurements were taken after the tunnel walls had been carefully smoothed down. In consequence, the friction factor ratio decreased substantially to f/f_s = 1.5–1.7. The results of these investigations are shown in figure 6 together with the theoretical values of the coefficient k/u^* calculated after the model presented in this paper, for the plate situated at the tunnel centre. Making allowance for different droplet size deposited on the plate, the weighted average of the deposition coefficient $\bar{k}/u^*$ was calculated as

$$\frac{\bar{k}}{u^*} = \frac{\sum_{dp} \frac{k}{u^*} d_p^3 \frac{\Delta N}{N_0}}{\sum_{dp} d_p^3 \frac{\Delta N}{N_0}} \quad [21]$$

where $d_p^3\, \Delta N/N_0$ stands for the mass fraction of the droplets of the diameter d_p in the total

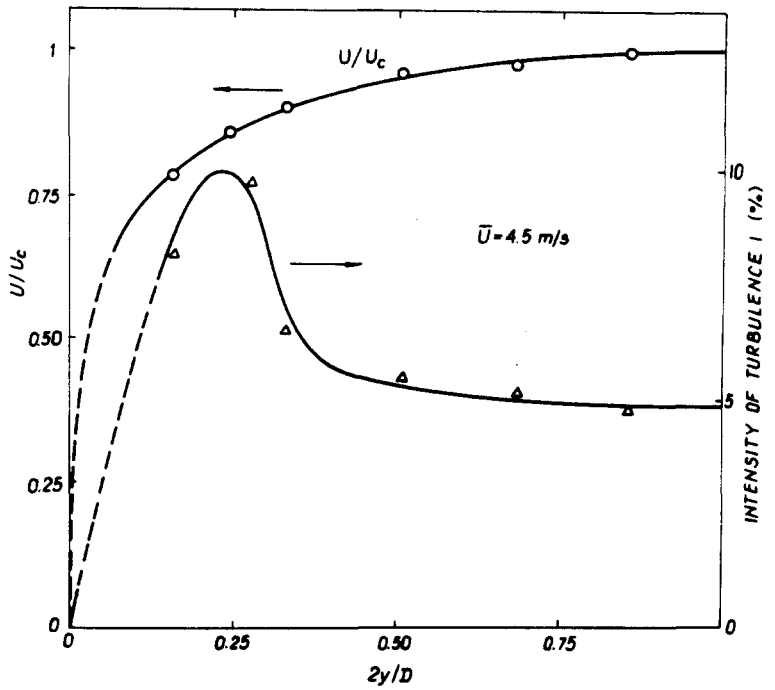

Figure 3. Intensity of turbulence and velocity distribution in the wind tunnel.

amount of droplets N_0. This fraction was determined from the droplet size measurements. In the calculations performed after the above formula [21] the relation [13] was used for droplets having dimensionless stopping distance S^+ larger than 20. Since in the spectrum of the deposited droplets there was always a slight fraction of droplets for which $S^+ < 20$, the relation

$$\frac{k}{u^*} = 3.25 \times 10^{-4} S^{+2} \qquad [22]$$

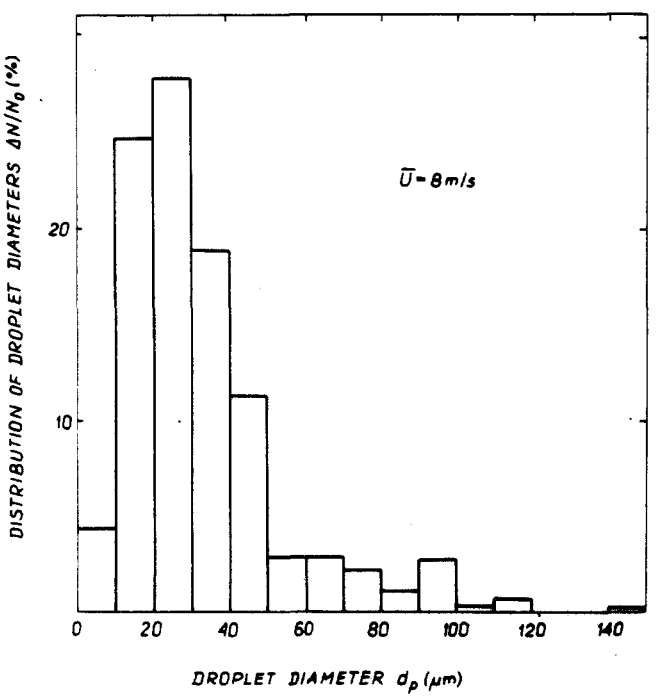

Figure 4. An example of droplet diameter distribution.

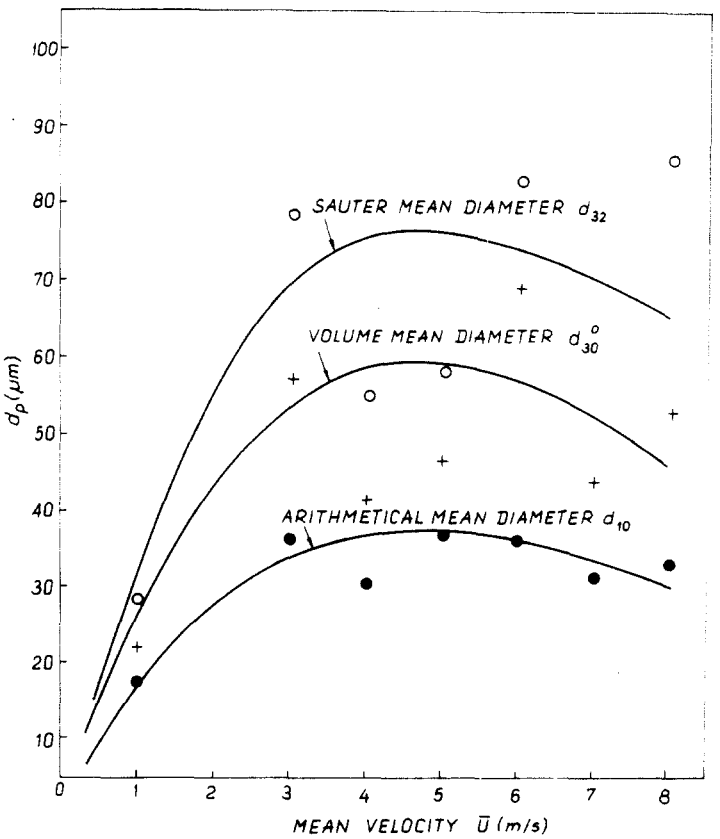

Figure 5. The effect of the mean velocity on the mean droplet diameters.

was used, which after McCoy & Hanratty (1977) best fills the experimental data for particles in the range $0.15 < S^+ < 22.9$.

However it holds for the deposition on the duct walls and hence its use for axially situated plates needs a certain correction. This may be done, for instance, by assuming for smaller droplets ($S^+ < 20$) the same distribution of the coefficient k/u^* as for larger ($S^+ > 20$), which is expressed by relation [15]. Finally in the calculations the following formula was used

$$\frac{k}{u^*} = 3.25 \times 10^{-4} S^{+2} \left(\frac{y^+}{S^+}\right)^{1.5/n} \qquad [23]$$

Calculations of the deposition coefficient made after [21] using the relationships [13] and [23] revealed that a more smooth curve of the deposition coefficient is obtained when the boundary value of the stopping distance S^+ is equal to 20 rather than 22.9 as suggested by McCoy & Hanratty (1977). This conclusion may be justified also due to the scatter in experimental data in McCoy & Hanratty (1977) figure 1.

Fingure 6 suggests a satisfactory agreement between the predicted and experimental values of the coefficient k/u^* for $Re_D > 80\,000$ ($S^+ > 20$), i.e. within the area of validity of the presented model. The theoretical and experimental values of the coefficient k/u^* rise very rapidly with increasing air velocity and reach a maximum value of about 0.15 at $Re_D \approx 80\,000$ and afterwards a slight decrease is observed. This is in agreement with the conclusion drawn by McCoy & Hanratty (1977) that for particles having $S^+ > 22.9$ the transfer coefficient appears to be insensitive to the particle diameter or fluid velocity.

The experimental results confirm also the conclusion drawn from [15] that the value of k/u^* is practically constant in the channel except in the region close to the wall, since actual

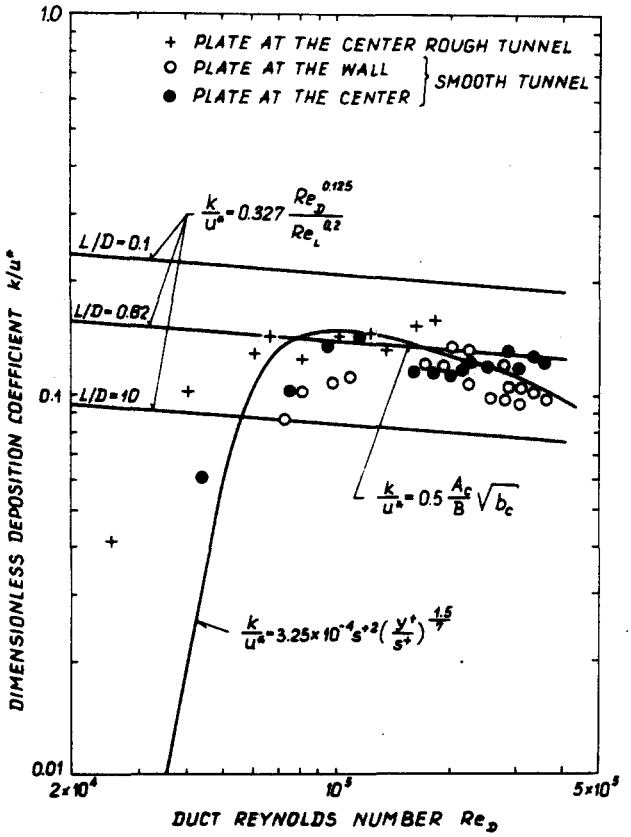

Figure 6. Comparison between theoretical and experimental values of k/u^*.

differences in the values of k/u^* for the plate at the channel centre and at the distance $y = 0.063$ m from the wall are small and lie within the measurement error range. For $Re_D > 80\,000$ the tunnel roughness did not affect the deposition coefficient.

The values of the deposition coefficient obtained in this study satisfactorily agree with those reported by McCoy & Hanratty (1977) and Cousins & Hewitt (1968). McCoy & Hanratty suggested $k/u^* = 0.17$ for particles with stopping distance larger than 22.9. The experiments made by Cousins & Hewitt (1968) on vertical tubes yielded $k/u^* \simeq 0.068$ for the 0.0318 m ($1^1/4''$) tube and $k/u^* = 0.095$ for 0.00953 m ($3^3/4''$) tube. Drop size measurement revealed the Sauter mean dia. d_{32} ranged from 40–70 μm for the smaller tube and 70–110 μm for the larger one. In the present study the Sauter mean dia. d_{32} varied within the same range as for the smaller tube (figure 5) and the transfer coefficient k/u^* was found to be very close to that of Cousins & Hewitt (1968).

For the sake of comparison the distribution of the coefficient k/u^* calculated after the method by Simpson & Brolls (1974) is also plotted in figure 6. When the simplest Reynolds analogy between heat and mass transfer is combined with the formula describing heat transfer on a plate and the boundary layer on the plate is assumed entirely turbulent due to the stirring action of the droplets the Simpson and Brolls model results in the relationship

$$\frac{k}{u^*} = 0.327 \frac{Re_D^{0.125}}{Re_L^{0.2}}. \qquad [24]$$

The calculations according to this formula were performed assuming the duct diameter $D = 0.365$ m and different values of the ratio L/D, where L is the plate length. Plate Reynolds number was calculated as $Re_L = 1.25 \bar{u} L \rho_G / \mu_G$. Even if the analogy between heat and mass

transfer in this case may be objected to, the results shown in figure 6 are in favour of this model at least as a first approximation for the region where the inertial deposition prevails.

5. SUMMARY

The paper presents the deposition model developed for particles having the dimensionless stopping distance S^+ larger than 20. The model assumes the existence of the boundary region of the thickness $y^+ = S^+$ where the large inertia particles do not follow the stream motion and are projected through it due to their initial velocity impulse gained at the edge of this region. The model allows determination of the deposition coefficient for a vertical plate situated in a duct at an arbitrary distance from the duct wall and also on the vertical duct wall itself.

The experiment confirmed the validity of this model in the range under investigation, i.e. for $Re_D = 8 \times 10^4$ to 36×10^4, corresponding approximately to the stopping distance range $S^+ = 20$–150 based on the mean droplet size $d_{30} = 45\ \mu$m.

REFERENCES

ALEXANDER, L. G. & COLDREN, C. L. 1951 Droplet transfer from suspending air to duct walls. *Ind. Engng Chem.* **43**, 1325–1331.

BEAL, S. K. 1970 Deposition of particles in turbulent flow on channel or pipe walls. *Nucl. Sci. Engng* **40**, 1–11.

COMTE-BELLOT, G. 1965 *Ecoulement Turbulent Entre Deux Parois Paralleles.* Pub. Sci. et Tech. du Ministere de L'air, No 418.

COUSINS, L. B. & HEWITT, G. F. 1968 Liquid phase mass transfer in annular two-phase flow: droplet deposition and liquid entrainment. *AERE-R* 5657.

FRIEDLANDER, S. K. & JOHNSTONE, H. F. 1957 Deposition of suspended particles from turbulent gas streams. *Ind. Engng Chem.* **49**, 1151–1156.

GANIC, E. N. & ROHSENOW, W. M. 1979 On the mechanism of liquid drop deposition in two-phase dispersed flow. *ASME J. Heat Transfer* **101**, 288–294.

HINZE, I. O. 1959 *Turbulence.* McGraw-Hill, New York.

HUTCHINSON, P., HEWITT, G. F. & DUKLER, A. E. 1971 Deposition of liquid or solid dispersions from turbulent gas streams: A stochastic model. *Chem. Engng Sci.* **26**, 419–439.

LIU, H. Y. & ILORI, T. A. 1974 Aerosol deposition in turbulent pipe flow. *Environ. Sci. Technol.* **8**, 351–356.

MCCOY, D. D. & HANRATTY, T. I. 1977 Rate of deposition of droplets in annular two-phase flow. *Int. J. Multiphase Flow* **3**, 319–331.

NAMIE, S. & UEDA, T. 1972 Droplet transfer in two-phase annular mist flow. *Bull. ISME* **15**, 1568–1580.

NAMIE, S. & UEDA, T. 1973 Droplet transfer in two-phase annular mist flow. *Bull. ISME* **16**, 752–764.

ROUHIAINEN, P. O. & STACHIEWICZ, J. W. 1970 On the deposition of small particles from turbulent streams. *ASME J. Heat Transfer* **92**, 169–177.

SCHLICHTING, H. 1955 *Boundary Layer Theory.* McGraw-Hill, New York.

SIMPSON, H. C. & BROLLS, E. K. 1974 Droplet deposition on a flat plate from an air/water mist in turbulent flow over the plate. *Symp. on Multi-Phase Flow System.* University of Strathclyde, Glasgow.

TRELA, M. 1980 Droplet deposition on a flat plate from an air/water turbulent mist flow (in Polish). *Report of the Institute of Fluid-Flow Machinery* 100/997/80.

TRELA, M. 1981 Deposition of droplets from turbulent stream. Submitted to *Wärme- und Stoffübertragung.*

APPENDIX A

The stopping distance

The boundary layer adjacent to a surface is characterized by the existence of fluctuations caused by the incursion of turbulent eddies from the turbulent core. However, such fluctuations are strongly damped in the vicinity of the wall. It is assumed that at a certain distance from the wall they exert little influence on the motion of the particles. Thus, the immediate wall region may be described as exerting only viscous drag on the particles. The equation of motion for such particles is thus

$$m_p \frac{du_p}{dt} = -fu_p \qquad [A1]$$

where the Stokes friction coefficient f is customarily used. The integration of [A1] gives

$$u_p = u_0 e^{-t/\tau} \qquad [A2]$$

and

$$X = u_0\tau(1 - e^{-t/\tau}) \qquad [A3]$$

for the velocity and displacement, respectively. The characteristic time $\tau = \rho_p d_p^2/18\mu_G$. As $t/\tau \to \infty$ the distance that the particle penetrates (stopping distance) is given by

$$S = \frac{\rho_p d_p^2 u_0}{18\mu_G}. \qquad [A4]$$

It is known that the Stokes law of friction is valid, in general, for $Re_p < 1$. This condition was satisfied in the experimental investigation. For example, at ambient temperature, for $d_p = 50\,\mu m$ and $Re_D = 10^5$ one obtains; $A = 0.7$, $u^* = 0.188\,m/s$, $b = 0.18$ and $\nu_G = 14 \times 10^{-6}\,m^2/s$.

Thus the droplet Reynolds number

$$Re_p = \frac{v_p' d_p}{\nu_G} = \frac{Au^*\sqrt{b}\,d_p}{\nu_G} = 0.2. \qquad [A5]$$

It is also easy to show that an error made when the Stokes law is applied for $Re_p > 1$ is relatively small. Following Simpson & Brolls (1974) the particle drag coefficient C_D (which is related to f) may be given by

$$C_{DS} = \frac{24}{Re_p} \quad \text{(Stokes law)} \quad \text{for} \quad Re_p \le 0.4207 \qquad [A6]$$

$$C_D = \frac{26.9}{Re_p^{0.8667}} \quad \text{for} \quad Re_p \ge 0.4207 \qquad [A7]$$

and, hence the error is determined by the ratio

$$\frac{C_D}{C_{DS}} = 1.12\,Re_p^{0.133} \qquad [A8]$$

The calculations prove that even at the Reynolds number as high as $Re_p = 10$ the actual value of drag coefficient is only 50% higher than that calculated by Stokes law.

This fact justifies the application of Stokes law at $Re_p > 1$. Some examples of such approach are the papers by McCoy & Hanratty (1977), Liu & Ilori (1974).

APPENDIX B

Deposition probability

Deposition probability may be expressed as a product

$$P = P_1 P_2 \qquad [B1]$$

where P_1 is the fraction of particles getting the velocity impulses towards the wall, P_2 is the fraction of particles reaching the wall due to these impulses. Deposition in circular channels is mainly controlled by the radial particle velocity fluctuations, thus P_1 equals 0.5. Determination of the probability P_2 is more complex. Since it has been assumed that the particles are insensitive to the eddies at $y < S$ then P_2 is inversely proportional to the probability of the particle collision with each other during "a free flight" to the wall. This, in turn, is proportional to the stopping distance and the particle concentration.

Trela (1981) showed that for a low particle concentration the probability P_2 decreases when the stopping distance S^+ increases. This fact may be expressed for $S^+ > 20$ by the relation

$$p_2 = aS^{+m} \qquad [B2]$$

where coefficients a and m equal 1.35 and -0.1, respectively. It is seen that P_2 slightly depends on the exponent m. Therefore for relatively low values of S^+ P_2 approximately equals 1.0 what leads to $P \simeq 0.5$.

APPENDIX C

Concentration profile

The approach presented in this paper resembles the integral analysis of the boundary layer where in order to get the shear stress (heat flux) at the wall one has to assume the velocity (temperature) distribution function in the boundary layer. It is shown by Schlichting (1955) that the quality of the results depends to a great extent on the assumptions which are made for this function.

If a rough approximation is desired, it is necessary to satisfy only the boundary conditions for the function. A good example is the use of power-law velocity profile in the analysis of the boundary layer although it has two obvious difficulties; the velocity gradients at the wall and that at δ are incorrect.

Beal (1970) used the power-law profile for particle concentration in the channel turbulent core. He has also showed that this assumption leads to the linear particle mass flux distribution in this region, what has been frequently used.